3D ANALYSIS OF MAGNETOHYDRODYNAMIC (MHD) MICROPUMP PERFORMANCE USING NUMERICAL METHOD

S. Derakhshan* **K. Yazdani**

School of Mechanical Engineering
Iran University of Science & Technology
Tehran, Iran

ABSTRACT

In the present study, a 3-dimensional model was developed to investigate fluid flow in MHD micropumps. Initially, 3D governing equations were derived and numerically solved using the finite volume method/SIMPLE algorithm. The case study was a (MHD) micropump built in the year 2000 (channel length: 20mm, channel width: 800μm, channel height: 380μm and electrode length: 4mm). The applied magnetic flux density was 13mT and the electric current was different for various solutions (10 ~ 140mA). The numerical results were verified by experimental and analytical data for several solutions. In addition effects of magnetic field strength, electric current,geometrical parameters of the MHD micropump, electrode length and electrode location on its performance have been investigated. Finally the results has been considered and discussed.

Keywords: Micropump, Magnetohydrodynamic (MHD), Lorentz force, Numerical analysis.

1. INTRODUCTION

Magnetohydrodynamic (MHD) is a phenomenon observed in electrically conductive liquid in the presence of a magnetic field [1]. When an electrical current passes through an electrically conductive fluid filled between two facing electrodes, in the presence of an external magnetic field applied on perpendicular to the direction of the current, a volumetricLorentz force is generated. This distributed volumetric force leads a pressure difference of the conductive fluid experiences that drives the fluid along the channel [2].

Recently the use of MHD to propel electrolyte solutions in microsystems has been reported. Jang and Lee were the first to use the MHD pumping in microchannels [3]. Lemoff and Lee demonstrated an AC MHD micropump which produces a continuous flow [4]. Huang *et al.* fabricated and tested a LIGA microfabricated pump based on a DC type MHD Principle. In this experiment research, bubble generation affected the flow rates for most potential. Average flow rates were not stable and finally decreased to zero for all solutions running for very long times. They concluded that if the direction of the supplied driving voltage could be reversed, the generated bubble would not be accumulated to affect the normal operation of the pump [5]. Zhong *et al.* fabricated a MHD pump with ceramic tapes [6]. Eijkel *et al.* designed a circular ac MHD micropump for chromatographic applications [7]. Nguyen and Kassegne reported a DC MHD micropump with bubble isolation and release system [8].

In addition, in the simulation and performance evaluation of these micropumps, a lot of works hasbeendone. Wang *et al.* simulated the two-dimensional fully developed laminar flow for a MHD micropump [9]. Ho studied a MHD pump analytically [10]. Chaabane *et al.* simulated a two-dimensional MHD flow to analyses pressure and velocity distribution for electrically conducting incompressible fluids [11]. Peng *et al.* studied on alternating magnetic field of MHD pump [12]. Duwairi and Abdullah investigated numerically the effect of Hartmann number on velocity and pressure [13]. Daoud and Kandev studied MHD by direct current electromagnetic pump for liquid aluminum [14]. Kabbani *et al.* introduce a new approximate solution for MHD flow in microchannels [15]. Rivero and Cuevas analyzed the slip condition in MHD micropumps [16]. Das *et al.* studied some practical applications of MHD pumping such as inject selective volume of reagent in reaction chamber [17]. Moghaddam studied MHD micropumping of power-law fluids. It was observed, the power-law exponent has a strong effect on the volumetric flow rate of MHD micropumps [18].

In the present study, initially, the governing equations of MHD micropumps were introduced. Solving the equations by numerical methods, the effects of magnetic field, electric current, channel dimensions, electrode length and electrode location on the performance of these micropumps were investigated.

2. MHD MICROPUMPS GOVERNING EQUATIONS

The fundamental equations of the MHD principle comprises two parts:

* Corresponding author (shderakhshan@iust.ac.ir)

DOI : 10.1017/jmech.2015.39
Copyright © 2015 The Society of Theoretical and Applied Mechanics, R.O.C.
https://doi.org/10.1017/jmech.2015.39 Published online by Cambridge University Press

• Electromagnetic

• Classical fluid dynamics

The electromagnetic governing equations are represented by the Maxwell's equations and the Ohm's law, while the classical fluid dynamics governing equations have been represented by the continuity equation and the Navier-Stokes equation. In order to solve these equations, steady electric and magnetic fields, laminar, steady and incompressible flow with constant flow properties are assumed. The reduced form of the MHD governing equations can be written as the Ohm's law, continuity equation and Navier-Stokes equation as follow:

Ohm's law:

$$\vec{J} = \sigma\left(\vec{E} + \vec{V} \times \vec{B}\right) \tag{1}$$

Volumetric Lorentz force:

$$\overrightarrow{F_L} = \left(\vec{J} \times \vec{B}\right) \tag{2}$$

Continuity equations:

$$\nabla \cdot \vec{V} = 0 \tag{3}$$

Navier-Stokes equations:

$$\rho\left(\vec{V} \cdot \nabla\vec{V}\right) = -\nabla p + \mu\nabla^2\vec{V} + F_L \tag{4}$$

where σ, ρ, μ, B, J, E, V and P, are electrical conductivity, fluid density, dynamic viscosity, magnetic flux density vector, current density vector, electric field vector, fluid velocity vector and pressure respectively.

3. DEVELOPMENT OF 3D MICROCHANNEL EQUATIONS

A MHD micropump consisted of a channel with length L, with rectangular cross-section width W and with height h, has been assumed including a full field electrolyte solution (Fig. 1). The placed electrodes on the side walls, are subjected to a potential difference V, therefore there is an electric field $\vec{E} = Ee_y$ ($E = V/w$). Also, a magnetic field $\vec{B} = Be_z$ is applied. The electric and magnetic fields of AC micropumps are alternating and they are expressed as $\vec{E} = E\sin(\omega t + \phi)\, e_y$ and $\vec{B} = B\sin(\omega t)\, e_z$ respectively, where ω is the angular frequency of the fields and φ is the phase angle between the electric and magnetic fields. Velocities in x, y and z directions are shown by u, v and w, respectively [19].

Then, Ohm's law is:

$$J_x = \sigma B v \tag{5}$$

$$J_y = \sigma(E - Bu) \tag{6}$$

$$J_z = 0 \tag{7}$$

Volumetric Lorentz force is:

$$F_{L_x} = J_y \times B = \sigma EB - \sigma B^2 u \tag{8}$$

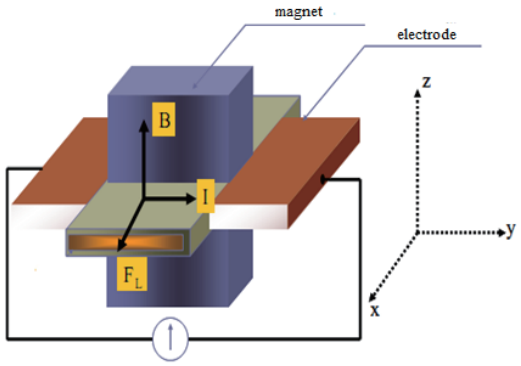


Fig. 1 A Schematic of a MHD micropump [20].

$$F_{L_y} = J_x \times B = -\sigma B^2 v \tag{9}$$

$$F_{L_z} = 0 \tag{10}$$

on the right of the relationship 8, the first term is Lorentz force in the flow direction and the second term is Lorentz force in the opposite direction of the flow (is called reverse Lorentz force).The expressed Lorentz forces are related to the DC MHD micropump. In AC MHD micropump, the time-averaged Lorentz force, used in Navier-Stokes equations, can be given by:

$$\overline{F} = \frac{\int_0^{2\pi} \vec{J}\times\vec{B}\, d\omega t}{2\pi} \tag{11}$$

Therefore the obtained velocity will be the average velocity.

3D Navier-Stokes and continuity equations can be written as follows:

$$\frac{\partial u}{\partial x} + \frac{\partial v}{\partial y} + \frac{\partial w}{\partial z} = 0 \tag{12}$$

$$\rho\left(u\frac{\partial u}{\partial x} + v\frac{\partial u}{\partial y} + w\frac{\partial u}{\partial z}\right) = -\frac{\partial p}{\partial x} + \mu\left(\frac{\partial^2 u}{\partial x^2} + \frac{\partial^2 u}{\partial y^2} + \frac{\partial^2 u}{\partial z^2}\right) + F_{L_x} \tag{13}$$

$$\rho\left(u\frac{\partial v}{\partial x} + v\frac{\partial v}{\partial y} + w\frac{\partial v}{\partial z}\right) = -\frac{\partial p}{\partial y} + \mu\left(\frac{\partial^2 v}{\partial x^2} + \frac{\partial^2 v}{\partial y^2} + \frac{\partial^2 v}{\partial z^2}\right) + F_{L_y} \tag{14}$$

$$\rho\left(u\frac{\partial w}{\partial x} + v\frac{\partial w}{\partial y} + w\frac{\partial w}{\partial z}\right) = -\frac{\partial p}{\partial z} + \mu\left(\frac{\partial^2 w}{\partial x^2} + \frac{\partial^2 w}{\partial y^2} + \frac{\partial^2 w}{\partial z^2}\right) + F_{L_z} \tag{15}$$

The boundary conditions can be specified as follows:

• Inlet: $P(0, y, z) = 0$

• Outlet: $\partial V/\partial x = 0$

• Walls: $V(x, 0, z) = 0$, $V(x, y, 0) = 0$, $V(x, W, z) = 0$, $V(x, y, h) = 0$

$P(0, y, z) = 0$, is the constant static pressure at inlet and $\partial V/\partial x = 0$ at outlet is the fully developed velocity profile.

https://doi.org/10.1017/jmech.2015.39 Published online by Cambridge University Press

4. NUMERICAL SETUP

In order to solve the equations numerically, the mesh should be generated in the computing region. The uniform mesh by rectangular elements was used for mesh generation in computing domain.

In various modes including different geometries, electric and magnetic fields, the mesh independency was controlled by solving different mesh sizes. The mesh sized 600,000 showed a difference less than 0.5% for the velocity and the pressure comparing to mesh sized 1,000,000 for the study micropump (length: 20mm, height: 380μm, width: 2200μm, electrical current: 140mA and magnetic flux: 20mT).

According to the coupling equations, an iterative solution method should be used to solve the equations. The SIMPLE algorithm was used to solve the equations based on control volume method. In this algorithm, by assuming pressure field, 3D full Navier-Stokes equations are solved to evaluate the velocity components u, v and w. Continuity equation must be satisfied by these obtained velocity components. If not, again Navier-Stokes equations should be solved by using the corrected pressure value and the process must be continued as long as the continuity equation is satisfied.

The necessary condition for convergence is given by:

$$\left|\frac{V^{new}-V^{old}}{V^{new}}\right| \leq \varepsilon \qquad (16)$$

where V is the desired variable and ε is the convergence criterion which is roughly equal to 10^{-4}.

5. VALIDATION

In order to verify the numerical method, the numerical results were compared with the experimental values provided by Lemoff and Lee for an AC MHD micropump [4].

The fabricated micropump by Lemoff and Lee has a channel length of 20mm, channel width of 0.8mm, channel height of 0.38mm and Electrode length of 4mm. Various solutions named 1M NaCl, 0.1M NaCl, 0.01M NaCl, 0.01M NaOH, PBS (pH 7.2) and Lambda DNA in 5mM NaCl were employed for the flow velocity experiments. The applied electric currents were set at 140, 100, 36, 24, 12 and 10mA, respectively, while the average AC magnetic flux density was kept at 13mT. For solutions, the electrical conductivity is 1.5s/m and its dynamic viscosity is 0.0006 Pa.s. It can be seen in Table 1 and Fig. 2, the coincidence between the present calculation results and the experimental data is satisfactory for the most solutions and the maximum deviation is less than 10%. The deviations between the present calculations and experimental data for the case of 0.1M NaCl solution is due to the experimental errors [4]. Also the present calculation results was compared with the analytical solutions for fully developed MHD flow. To this end, the proposed relationship by Kabbani *et al.* [15] was used. it observed that the analytical solutions and present three-dimensional analysis results are very close together.

Table 1. Comparison of mean flow velocity value of the present calculation, analytical solution and experimental results for different solutions.

Solution	Flow Velocity (mm/s)		
	Experiments [4]	Analytical [15]	Present Study
1M NaCl	1.51	1.682	1.66
0.1M NaCl	0.51	1.2	1.198
0.01M NaCl	0.34	0.433	0.436
0.01M NaOH	0.3	0.288	0.296
PBS PH 7.2	0.16	0.144	0.153
Lambda DNA in 5 mMNaCl	0.11	0.12	0.12

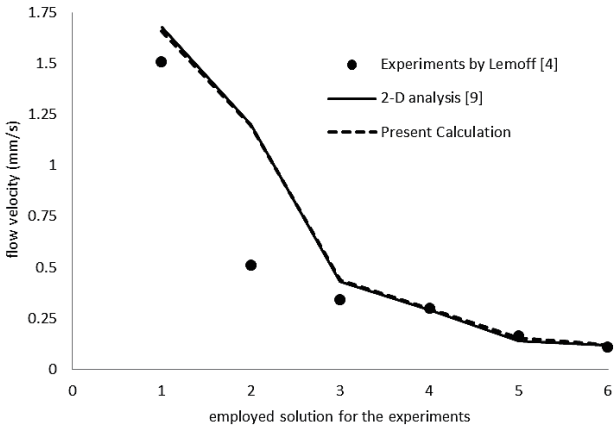


Fig. 2 Comparisons between the present calculation, analytical and experimental results.

6. RESULTS AND DISCUSSIONS

In this section, after considering the numerical results, the effect of various parameters on the MHD micropump performance has been investigated.

6.1 Numerical Simulation Results

Figure 3 shows the changes of the flow velocity in channel. While the Reynolds number is low, the entrance length is small. Figure 4 shows the velocity profile of developed domain in the channel cross section. It can be seen the velocity profile is parabolic and the maximum value of velocity is in the channel center.

According to Eqs. (13) to (15), there is a source term named Lorentz force applied in zone B. This is obvious that the effect of the source term can be seen as increasing static pressure of the fluid, exactly like axial pumps which the propeller do work on fluid by increasing its static pressure without no reversed flow.

Figure 5 shows the changes of the pressure in the x direction. The pressure distribution in the x direction can be divided into three zones: A, B and C. Fluid moves in the MHD micropump as a result of the Lorentz force which is applied in zone B. In zones A and

https://doi.org/10.1017/jmech.2015.39 Published online by Cambridge University Press

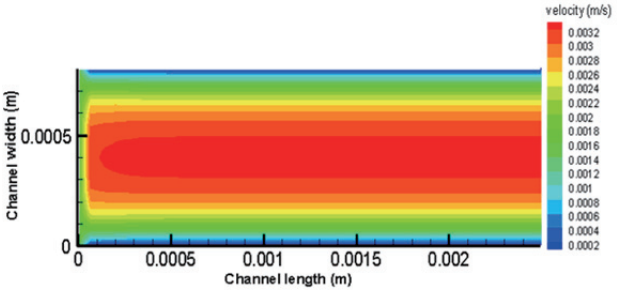


Fig. 3 Variation of velocity component u along the channel.

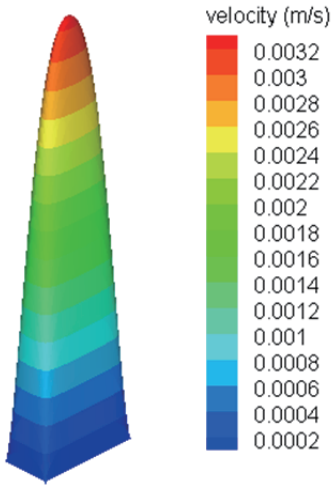


Fig. 4 Profile of the velocity component u in the channel cross-section.

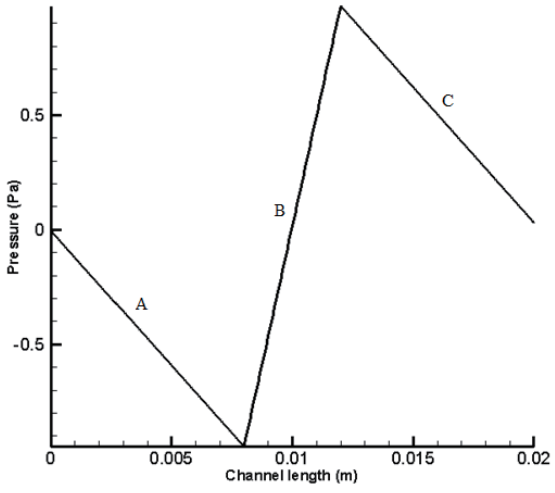


Fig. 5 Variation of pressure along the channel.

C, the fluid moves as a result of the induced pressure gradient therefore in these zones the pressure gradient is negative. The zone B is affected by the Lorentz force and this force causes the fluid motion in zone B. In this zone, the pressure gradient is positive and the pressure increases.

6.2 Magnetic Field Strength

One of the important parameters affecting the performance of the magnetohydrodynamicmicropump is the magnetic field strength. The generated Lorentz force in the streamwise x-direction is directly proportional to the strength of the magnetic field and the Lorentz force increases by increasing the magnetic field strength. Figure 6 shows the changes of the Lorentz force with the magnetic field strength in the electric currents of 36, 100 and 140mA. As can be seen, the Lorentz force increases linearly by increasing the magnetic field while the lines slope is more in larger electric currents.

The magnetic field strength has an effect on the reverse Lorentz force. The reverse Lorentz force is proportional to the square of the magnetic field strength. Figure 7 illustrates the changes of the reverse Lorentz force by the magnetic field strength in different electric currents. The values of the reverse Lorentz force are very small. In the Low magnetic fields strength, the values of the reverse Lorentz force in different electric currents are close together and the force values increases by increasing the magnetic field strength while the changes is more in the larger electric currents.

6.3 Electric Current

Another parameter affecting the performance of the magneto hydrodynamic micropump is electric current. The generated Lorentz force in MHD micropump is directly proportional to the electric current. Figure 8 shows the changes of the Lorentz force with the electric current in magnetic fields of 5, 13 and 20mT. As can be seen, the Lorentz force increases linearly with the electric current.

Figure 9 illustrates the changes of the reverse Lorentz force with the electric current in different magnetic fields. the reverse Lorentz force increases linearly by increasing the electric current, Because of the reverse Lorentz force is directly proportional to the flow velocity and since the velocity increases with the electrical current, so the reverse Lorentz force increases by increasing the electric current.

6.4 Channel Size

The channel size is the important parameter that they have an effect on the fluid flow in MHD micropumps including the length, width and height of channel. The Lorentz force is independent on the channel width.

In Fig. 10, the changes of the reverse Lorentz force with the channel width in electric current of 140mA and various magnetic fields is shown. In small magnetic fields, the reverse Lorentz force slightly increases by increasing the channel width, but in larger magnetic fields, the force values has increased significantly by increasing the channel width.

Figure 10 illustrates the effect of channel width on the velocity profiles in the electric current of 140mA and the magnetic field of 13mT. The velocity increases by increasing the channel width. First, by increasing the channel width of 400μm, the changes of the velocity is very much, but the changes is low in larger channel width. When the channel width is larger than 1500μm, any increasing in the channel width,

https://doi.org/10.1017/jmech.2015.39 Published online by Cambridge University Press

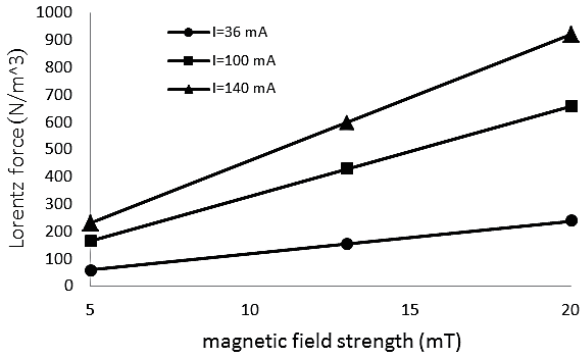


Fig. 6 Variation of Lorentz force with the magnetic field strength at different electric currents.

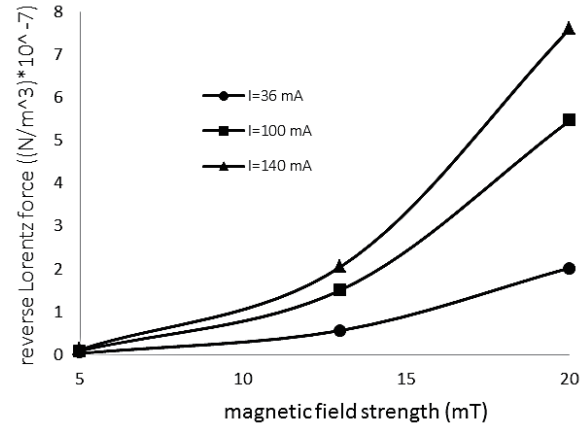


Fig. 7 Variation of reverse Lorentz force with the magnetic field strength at different electric currents.

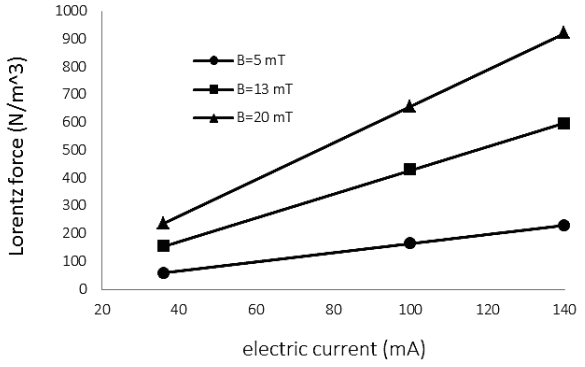


Fig. 8 Variation of Lorentz force with the electric current at different magnetic fields.

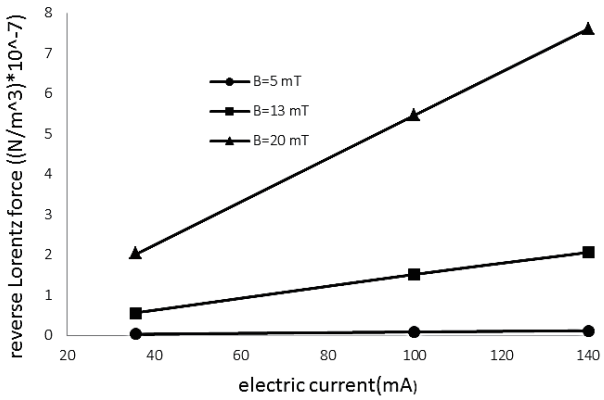


Fig. 9 Variation of reverse Lorentz force with the electric current at different magnetic fields.

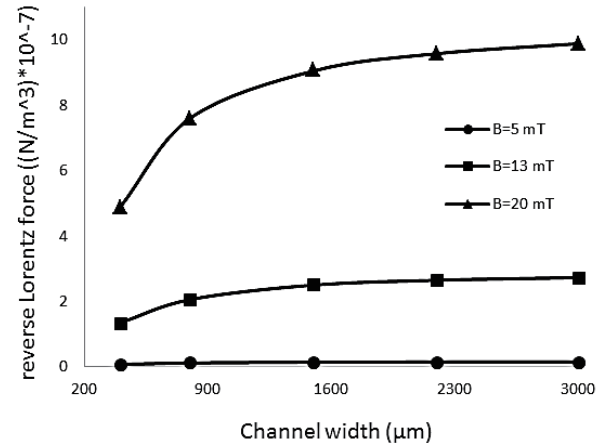


Fig. 10 Variation of reverse Lorentz force with the channel width in various magnetic fields.

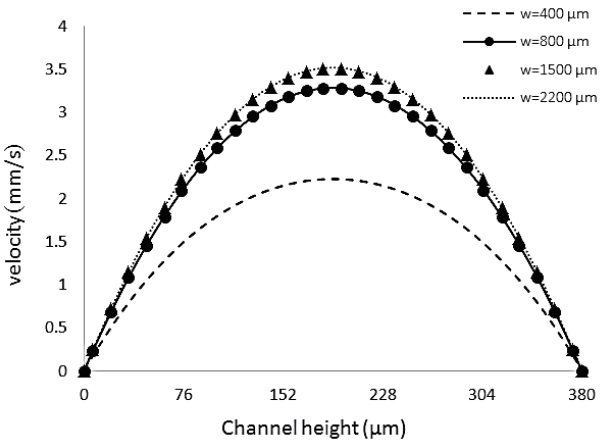


Fig. 11 Variation of flow velocity with the channel height in various channel widths.

would not affect on the flow velocity and the velocity profiles are almost overlapped. This matter is due to the fact that the effect of the walls friction on the velocity decreases by increasing the channel width.

As can be seen in Fig. 11, the velocity increases by increasing the channel width, thus the reverse Lorentz force that is proportional to the velocity (According to Eq. (8)), increases by increasing the channel width.

Figure 12 shows the changes of the Lorentz force with the channel height in the electric current of 140mA and different magnetic fields. The Lorentz force decreases by increasing the channel height due to the decrease of the electric current density. Initially by increasing the channel height of 200μm, the decrease of the Lorentz force is large but the changes rate of the Lorentz force is less with further increase of the channel height.

Figure 13 shows the changes of the reverse Lorentz force with the channel height in electric current of 140mA and different magnetic fields. First, in a given magnetic field, the reverse Lorentz force increases by

https://doi.org/10.1017/jmech.2015.39 Published online by Cambridge University Press

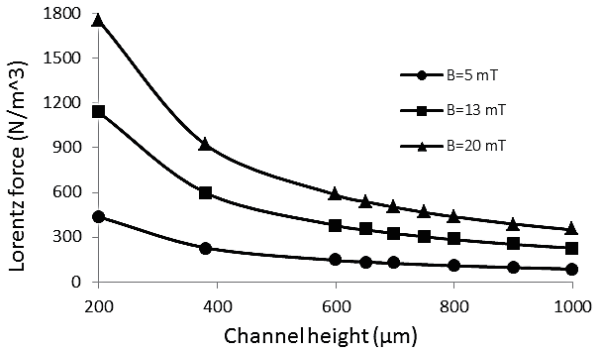


Fig. 12 Variation of Lorentz force with the channel height at different magnetic fields.

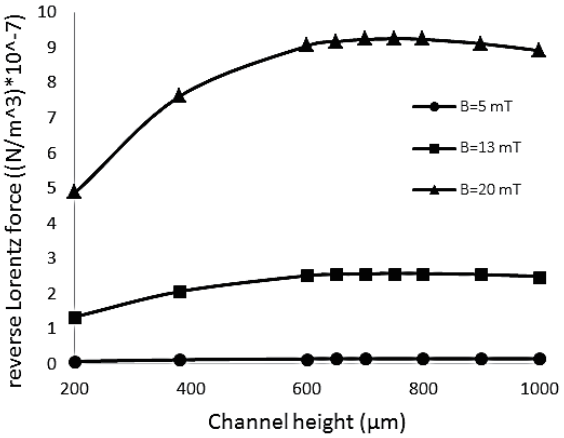


Fig. 13 Variation of reverse Lorentz force with the channel height in various magnetic fields.

increasing the channel height but more increasing the channel height leads to a decrease in the reverse Lorentz. Also it will be observed that the changes of the reverse Lorentz force versus the channel height, is more in larger magnetic fields.

Figure 14 illustrates the effect of channel height on the velocity profiles in the electric current of 140mA and the magnetic field of 13mT. First, by increasing the channel height of 200μm, the velocity increases but it decreases when the channel height is larger than 800μm. In fact, increasing in the channel height reduces the friction of channel walls and therefore the flow velocity increases. On the other hand, the surface area of electrodes increases by increasing the channel height and therefore the electric current density decreases, therefore the flow velocity reduces.

The average velocity decreases by increasing the channel length. the calculated flow velocities for channel lengths of 16mm, 20mm, 24mm and 28mm are, respectively, 2.05mm/s, 1.663mm/s, 1.394mm/s and 1.198mm/s. Figure 15 shows the velocity profiles in the middle section of the channel width for various values of the channel length. The values of the velocity decrease by increasing the channel length. As can be seen in Fig. 16, the pressure gradient in A and C zones is reduced by increasing the channel length because the lengths of these zones is increased. It means the pressure was changed more in zones with more lengths from 16mm to 28mm.

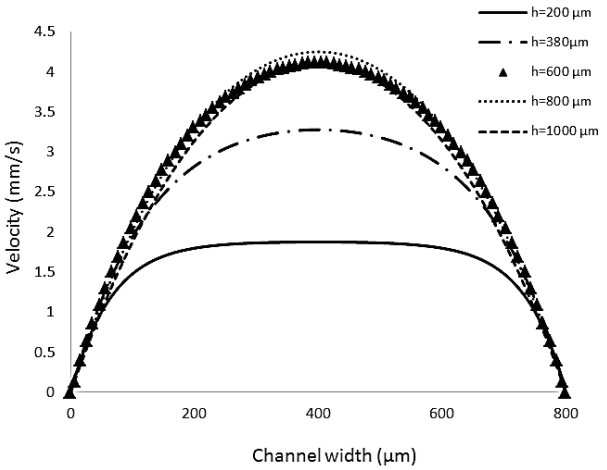


Fig. 14 Variation of flow velocity with the channel width in various channel heights.

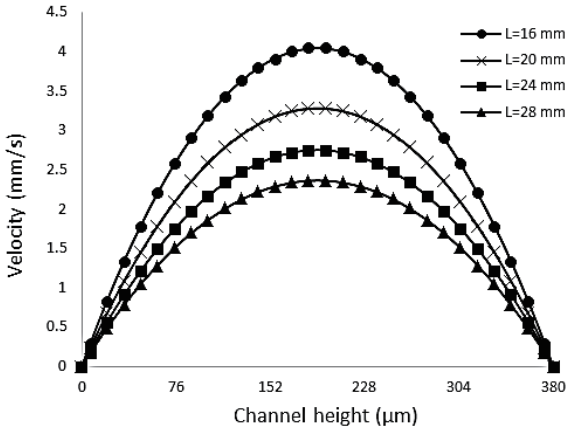


Fig. 15 Variation of flow velocity with the channel height in various channel lengths.

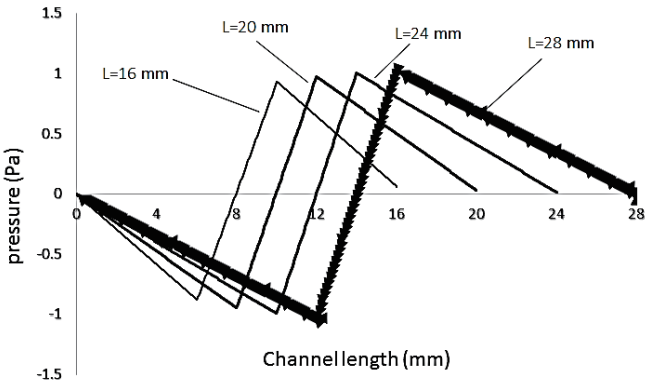


Fig. 16 Variation of pressure along the channel in various channel lengths.

The channel length changes do not affect the Lorentz force but it has an effect on the reverse Lorentz force (Fig. 17). The reverse Lorentz force decreases by increasing the channel length due to the reduction of the flow velocity. The volumetric Lorentz force is applied just in zone B, where the length of this zone is assumed constant and the meaning of changing channel length is changing zones A and C length.

https://doi.org/10.1017/jmech.2015.39 Published online by Cambridge University Press

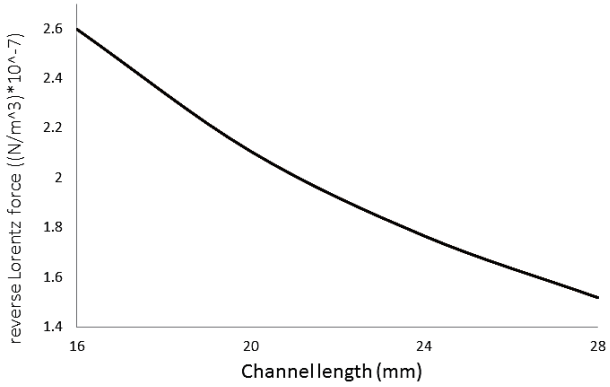


Fig. 17 Variation of reverse Lorentz force with the channel length.

6.5 Electrode Length

In order to investigate the effect of electrode length on the micropump performance, eight various electrode lengths were selected and the Lorentz force and average velocity were calculated for them. Figure 18 shows the effect of electrode length on the Lorentz force in electric current of 140mA and the magnetic field of 13mT. The Lorentz force decreases by increasing the electrode length from 2 to 14mm due to the reduction of the electric current density. It will be observed that the changes of the Lorentz force are high for small electrode lengths and low for larger one. Due to constant pressure gradient along the channel (Fig. 19), the changes of the average velocity with the electrode length are negligible. Volumetric Lorentz force is in relation with electric current per unit surface of electrode, so by increasing electrode length this force decreases but it affects on flow in a larger length. Thus this two effects compensate each other which result in constant Lorentz force.

As can be seen in Fig. 18 the Volumetric Lorentz force decreases by increasing the electrode length, thus in Fig. 1, the pressure values in zone B decreases by increasing the electrode length but in zones A and C that the length is decreased by increasing the electrode length, the pressure gradient is constant.

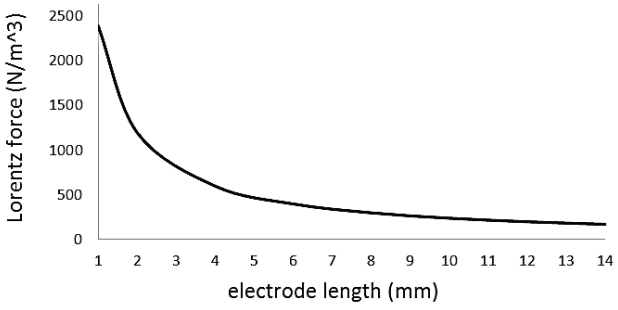


Fig. 18 Variation of Lorentz force with the electrode length (x).

Meanwhile, in this study, the electrodes were placed in several locations of the channel and its effect on the flow velocity was investigated. The electrodes were placed at a distance of 5.33 to 10.67mm from the channel inlet. The values of the pressure gradient along the channel keep constant by varying the electrode location in channel (Fig. 20). Therefore the values of the flow velocity are constant by changing the electrode location too.

The volumetric Lorentz force is constant by varying the electrode location, thus as can be seen in Fig. 20 the pressure gradient in three zones is constant.

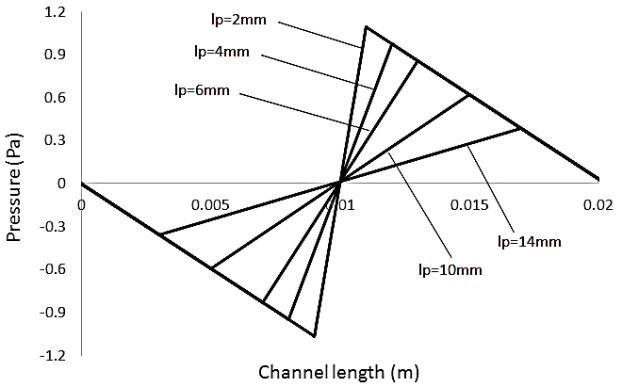


Fig. 19 Variation of pressure along the channel at different electrode lengths (l_p).

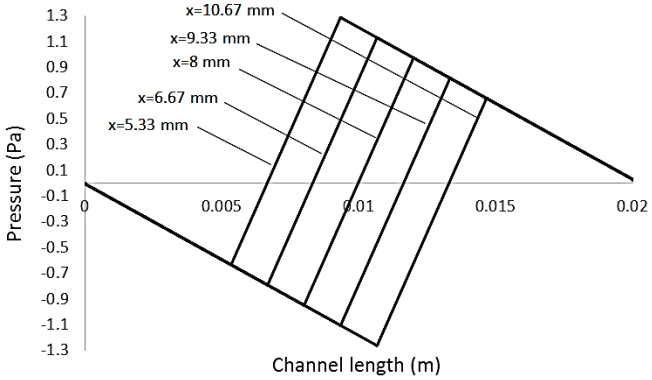


Fig. 20 Variation of pressure along the channel at different locations of the electrode in channel (x).

7. CONCLUSIONS

In this study, three-dimensional governing equations in MHD micropumps were developed and then were numerically solved using finite volume method/SIMPLE algorithm. Results showed that the entrance length is small and the pressure distribution in channel can be divided into three zones. The magnetic field strength and the electric current affected the values of the Lorentz force. This force increased by increasing the magnetic field and electric current. Therefore the flow velocity increased. It was also observed that the cross-sectional dimensions of the channel affected the MHD micropump performance. The volumetric Lorentz force was independent of the channel width but

https://doi.org/10.1017/jmech.2015.39 Published online by Cambridge University Press

it decreased by increasing the channel height. The fluid flow velocity increased by increasing the channel width. However, the changes of the flow velocity decreased for more values of the channel width. Meanwhile, increasing the channel width, did not affect the flow velocity. Initially, the flow velocity increased by increasing the channel height but more increasing the channel height decreased the flow velocity. Therefore, an optimal height of the channel could be determined. In addition, amounts of pressure gradient and the velocity along the channel reduced by increasing the channel length. The channel length had no effect on the Lorentz force. However, the reverse Lorentz force decreased by increasing the channel length.

Moreover, the effects of the electrode length and electrode location in channel on the micropump performance were evaluated. The results showed that the volumetric Lorentz force decreased by increasing the electrode length. Nevertheless, the values of the flow velocity is not changed. Also it was observed that the electrode location in channel had no effect on the flow velocity.

ACKNOWLEDGEMENTS

The authors gratefully acknowledge the support of and the contribution of the Iran University of Science & Technology.

REFERENCES

1. Patel, V. and Kassegne, S. K., "Electroosmosis and Thermal effects in Magnetohydrodynamic (MHD) Micropumps Using 3D MHD Equations," *Sensors and Actuators B*, **122**, pp. 42–52 (2007).
2. Lee, D. E., "Development of Micropump for Microfluidic Applications," Ph.D. Dissertaion, Department of Mechanical Engineering, Louisiana State University, Louisiana, U.S.A. (2007).
3. Jang, J. and Lee, S. S., "Theoretical and Experimental Study of MHD (Magnetohydrodynamic) Micropump," *Sensors and Actuators A*, **80**, pp. 84–89 (2000).
4. Lemoff, A. V. and Lee, A. P., "An AC Magnetohydrodynamic Micropump," *Sensors and Actuators B*, **63**, pp. 178–185 (2000).
5. Huang, L. *et al*., "LIGA Fabrication and Test of a DC Type Magnetohydrodynamic (MHD) Micropump," *Microsystem Technologies*, **6**, pp. 235–240 (2000).
6. Zhong, J., Yi, M., and Bau, H. H., "Magnetohydrodynamic (MHD) Pump Fabricated with Ceramic Tapes," *Sensors and Actuators A*, **96**, pp. 59–66 (2002).
7. Eijkel, J., *et al*., "A Circular AC magnetohydrodynamic Micropump for Chromatographic Applications," *Sensors and Actuators B*, **92**, pp. 215–221 (2003).
8. Nguyen, B. and Kassegne, S. K., "High-Current Density DC magenetohydrodynamics Micropump with Bubble Isolation and Release System," *Microfluidics and Nanofluidics*, **5**, pp. 383–393 (2008).
9. Wang, P. J., Chang, C. Y., and Chang, M. L., "Simulation of two-Dimensional Fully Developed Laminar Flow for a Magneto-Hydrodynamic (MHD) Pump," *Biosensors and Bioelectronics*, **20**, pp. 115–121 (2004).
10. Ho, J.-E., "Characteristic Study of MHD Pump with Channel in Rectangular Ducts," *Journal of Marine Science and Technology*, **15**, pp. 315–321 (2007).
11. Chaabane, R., Bouras, A., and Ben Nasrallah, S., "Numerical Magneto Hydro Dynamic Flow Simulation of Velocity and Pressure for Electrically Conducting, Incompressible Fluids," *Journal of the Brazilian Society of Mechanical Sciences and Engineering*, **29**, pp. 299–306 (2007).
12. Peng, Y., *et al*., "Experimental Study on Alternating Magnetic Field Magnetohydrodynamic Pump," *Journal of Hydrodynamics Series B*, **20**, pp. 591–595 (2008).
13. Duwairi, H. and Abdullah, M., "Numerical Computation of Fluid Flow in a Magnetohydrodynamic Micropump," *Turkish Journal of Engineering &. Environmental Science*, **32**, pp. 1–5 (2008).
14. Daoud, A. and Kandev, N., "Magneto-Hydrodynamic Numerical Study of DC Electromagnetic Pump for Liquid Metal," *Proceedings of the Comsol Conference*, U.S.A. (2008).
15. Kabbani, H. S., *et al*., "Analytical Prediction of Flow Field in Magnetohydrodynamic-Based Microfluidic Devices," *Journal of Fluids Engineering*, **130**, pp. 1–6 (2008).
16. Rivero, M. and Cuevas, S., "Analysis of the Slip Condition in Magnetohydrodynamic (MHDM) Icropumps," *Sensors and Actuators B*, **166**, pp. 884–892 (2012).
17. Das, C., Wang, G., and Payne, F., "Some Practical Applications of Magnetohydrodynamic Pumping," *Sensors and Actuators A*, **201**, pp. 43–48 (2013).
18. Moghaddam, S., "MHD Micropumping of Power-Law Fluids: A Numerical Solution," *Korea-Australia Rheology Journal*, **25**, pp. 29–37 (2013).
19. DePuy, T. R., "Fluid Dynamics and Heat Transfer in a Hartmann Flow," M.S. Thesis, Department of Mechanical Engineering, Rensselaer Polytechnic Institute, New York, U.S.A. (2010).
20. Tawk, M., "Etude Etréalisation d'un Système de Refroidissement Pour L'électronique de Puissance Basésur la Mise en Mouvement d'un Fluide Conducteur E'lectrique," Ph.D. Dissertation, Department of Engineering Science, University of Grenoble, Grenoble, France (2011).

(Manuscript received August 27, 2014,
accepted for publication January 29, 2015.)

https://doi.org/10.1017/jmech.2015.39 Published online by Cambridge University Press